Microscopic study of impurity resonance and tunneling magnetoresistance of nanoscale junctions

Yuan Ren, Zheng-zhong Li, Ming-wen Xiao, and An Hu
National Laboratory of Solid State Microstructures and Department of Physics, Nanjing University, Nanjing 210093, China

(Received 5 March 2006; revised manuscript received 17 November 2006; published 23 February 2007)

In this paper, we present a microscopic study of impurity resonance and tunneling magnetoresistance (TMR) for nanojunctions. We employ the Green's-function method to derive the tunneling wave functions and TMR from the spintronic model with nonmagnetic impurities and at a finite bias voltage. The analytical expressions for both direct and impurity-resonance tunnelings are obtained, where the lateral effect has been included. Within this framework, the TMR can be determined directly by the basic quantities of the junction, e.g., the position and the energy level of the impurity, the height and width of the barrier, the Fermi level and polarization of the electrodes, as well as the applied voltage. If the cross sectional area of the junction gets very small, we find that it is the impurity resonance and the quantum-coherence effect that control the bias dependence of TMR: the impurity resonance makes the TMR change from positive to negative, and the quantum-coherence effect decreases the TMR as the bias voltage increases. The experimental results of TMR for the junctions with the area smaller than 0.01 μm^2 can then be explained naturally. We also find that the direct and impurity-resonance tunnelings will compete with each other when the area of the junction is enlarged. Taking into account both the contributions of direct tunneling and impurity-resonance tunneling, the total TMR agrees quite well with the more recent experiments on the larger-area nanojunctions.

DOI: 10.1103/PhysRevB.75.054420 PACS number(s): 72.25.−b, 85.75.Mm, 85.75.−d, 73.63.Rt

I. INTRODUCTION

The tunneling magnetoresistance (TMR) occurring in magnetic tunnel junctions has attracted intensive attention since it was observed and studied by Jullière.[1] According to Jullière theory, the TMR is positive and independent of the barrier parameters. However, in 1999 Fert's group found that even though the electrodes are kept the same, when the Al_2O_3 barrier is replaced by the $SrTiO_3$ barrier, the TMR will change from positive to negative,[2] which indicates that the TMR depends explicitly on the insulating barrier. They interpreted these results in terms of interface chemical bonding proposed earlier by Tsymbal *et al.*[3] The details and the related references up to 2003 can be found in a recent comprehensive review.[4] Furthermore, Sharma *et al.*[5] revealed that the TMR in the Ta_2O_5-barrier junction can change from positive to negative when the bias voltage increases above several hundreds of millivolts. To explain this sign change of TMR under applied voltage, Li *et al.*[6] extended the Slonczewski model[7] from the zero-bias case to the finite bias case and found that there exists a bias-dependent quantum-coherence factor controlling the sign of the TMR. With this theory, the sign change of TMR can be explained qualitatively.

The magnetic tunnel junctions mentioned above belong to the common case, where the cross sections of junction are typically a fraction of mm^2 and the sign-change behaviors are produced by the direct tunneling and its quantum coherence.[6,8] If the cross section of the junction is reduced to the nanoscale, there can arise another type of sign-change behavior of TMR. By fabricating the junctions with cross sections smaller than 0.01 μm^2, Tsymbal *et al.*[9] found that TMR can be inverted at a very low bias voltage (about tens of millivolts) or even under the zero bias case. This inversion of TMR is ascribed to the scattering of the impurities localized in the barrier region. According to Ref. 9, three different kinds of bias dependence of TMR are observed when the energy of the localized state E_i varies. First, if E_i lies at the Fermi level E_F, the scattering resonance occurs and the TMR becomes negative near zero bias. Second, if E_i lies above and close to the E_F, but not close enough to invert the TMR at zero bias, the inversion can occur at a finite but small bias. Third, if E_i lies above and far from E_F, there is no TMR inversion, the TMR decreases with bias but remains positive within the measurable range of the applied voltage. Within a simple one-dimensional picture of impurity-resonance tunneling, they tried to simulate the experimental results using a phenomenological Breit-Wigner formula,[10]

$$G_{\sigma_L\sigma_R}(E) = \frac{2e^2}{\pi\hbar}\frac{\Gamma_{L\sigma_L}\Gamma_{R\sigma_R}}{(E-E_i)^2+(\Gamma_{L\sigma_L}+\Gamma_{R\sigma_R})^2}, \qquad (1.1)$$

where $\Gamma_{L\sigma_L}$ and $\Gamma_{R\sigma_R}$ correspond respectively to left and right half linewidths of the impurity resonance, and are taken as phenomenologically adjustable parameters in the simulation. It is found that the first case can be simulated quite well by Eq. (1.1).[9] As to the second case, Eq. (1.1) fails to reproduce the drop of TMR occurring at negative bias voltage. For the third case, no simulation has been given.

Following Tsymbal *et al.*, experiments are also performed with large-area nanojunctions, where the cross sections of the junction range from several μm^2 to hundreds of μm^2.[11,12] The results indicate that the TMRs show similar but different behaviors, in comparison to those of Ref. 9. However, the authors still simulate their experimental data with the one-dimensional phenomenological formula of Eq. (1.1), but pay no attention to the influence of enlarging on the cross section.[11,12] Obviously, owing to the scattering of impurity, the tunneling itself becomes three dimensional. The one-dimensional formula is insufficient and not suitable for the interpretation of TMR. Therefore a three-dimensional theory

 ©2007 The American Physical Society

must be proposed to include the lateral effect of cross section and the competition of direct and indirect tunnelings.

Theoretically, Vedyayev and co-workers[13,14] and Sheng *et al.*[15] have studied the impurity resonance and TMR in magnetic nanojunctions. However, in Ref. 15, only the zero-bias case was considered, therefore the result cannot account for the bias effect of impurity-resonant tunneling. The *I-V* characteristics and the diode effect were considered in Ref. 14. As to Ref. 13, the impurity-resonant tunneling result for the finite-bias case, i.e., Eq. (20) of Ref. 13, is conspicuously questionable. Therefore a microscopic theory suitable for the finite bias case is still needed.

The purpose of this paper is to present a microscopic theory to account for the impurity-resonant tunneling at finite bias, by using the method of Airy functions. The theory will itself be three dimensional, the lateral effect of the junction being included. It is shown that the direct tunneling and the indirect tunneling via impurity scattering will compete with each other if the cross section changes. Different from Refs. 9, 11, and 12 where the linewidths $\Gamma_{L\sigma_L}$ and $\Gamma_{R\sigma_R}$ are treated as constant parameters, the resonance linewidths in this paper will be derived from the basic quantities of the magnetic tunnel junction. We find that recent experiments[9,11,12] on impurity-assisted TMR can be explained naturally within this theory.

The rest of this paper is organized as follows. In Sec. II, we shall first present the spintronic tunneling model for the TMR of magnetic tunnel junctions, and then study the propagation of the tunneling electrons via Green's functions. In Sec. III, we explore for the direct and the indirect tunnelings, and concentrate mainly on their competition when the cross section of the junction is changed. In Sec. IV, we present our numerical results, and discuss in detail the impurity resonance and the lateral effect on TMR. Finally, we shall summarize our results briefly in Sec. V.

II. SPINTRONIC TUNNELING MODEL

In this paper, we shall consider a tunnel junction that consists of two identical FM electrodes and an insulating barrier. Within the barrier, random nonmagnetic impurities are distributed. As in Refs. 6 and 8, the ferromagnetic (FM) electrodes will be described using the single electron model with two parabolic spin bands. The Hamiltonian of the system has the form

$$H = H_0 + H_{\mathrm{imp}}, \tag{2.1}$$

where

$$H_0 = -\frac{\hbar^2}{2m}\nabla^2 + \phi(z), \tag{2.2}$$

$$H_{\mathrm{imp}} = \sum_i v(\mathbf{r} - \mathbf{r}_i) \tag{2.3}$$

with $\phi(z)$ the longitudinal potential,

$$\phi(z) = \begin{cases} -\sigma_{\mathrm{L}}\Delta, & z < 0, \\ \phi_0 - \dfrac{z}{d}eV, & 0 \leqslant z \leqslant d, \\ -\sigma_{\mathrm{R}}\Delta - eV, & z > d. \end{cases} \tag{2.4}$$

Here m is the effective mass of a tunneling electron, $v(\mathbf{r}-\mathbf{r}_i)$ is the scattering potential of the impurity at site $\mathbf{r}_i$, V is the applied voltage, d is the barrier width, ϕ_0 is the barrier height, Δ is the half exchange splitting between the two spin bands of the FM electrodes. The σ_{L} ($\sigma_{\mathrm{L}}=\pm 1$) and σ_{R} ($\sigma_{\mathrm{R}}=\pm 1$) denote the spin states of the electron in the left and right FM electrodes, respectively. In order to get a qualitative explanation on the bias-dependent TMR more directly, we simply adopt the potential profile within the barrier under bias to be a linear function of z (i.e., the trapezoidal shape)[6,8] instead of performing the exactly self-consistent calculations based on the nonequilibrium Green's-function formalism.[16]

To calculate the tunneling magnetoresistance, we employ the retarded Green's function (GF) to study the propagation of the electrons. For an incident electron from the left electrode, its transmission state in the right electrode can be given via GF as follows:[17]

$$\psi_{\mathrm{R}\sigma_{\mathrm{R}}}(\mathbf{r}) = i\int d\mathbf{r}'\int\frac{dE}{2\pi}G_{\sigma_{\mathrm{L}}\sigma_{\mathrm{R}}}(E;\mathbf{r},\mathbf{r}')\psi_{\mathrm{L}\sigma_{\mathrm{L}}}(\mathbf{r}'),$$
$$(z' \leqslant 0,\ z \geqslant d), \tag{2.5}$$

where $\psi_{\mathrm{L}\sigma_{\mathrm{L}}}(\mathbf{r}')$ is the initial stationary state of the incident electron with spin σ_{L}, $\psi_{\mathrm{R}\sigma_{\mathrm{R}}}(\mathbf{r})$ is the final (i.e., transmission) state of the electron with spin σ_{R}, and $\mathrm{G}_{\sigma_{\mathrm{L}}\sigma_{\mathrm{R}}}(E;\mathbf{r},\mathbf{r}')$ is the retarded Green's function in energy space. Equations (2.3) and (2.4) show that the scattering is elastic therefore the energy is conserved with respect to the initial and final states in Eq. (2.5).

We shall treat the impurity scattering H_{imp} as a perturbation to the basic Hamiltonian H_0. As a result, $G_{\sigma_{\mathrm{L}}\sigma_{\mathrm{R}}}(E;\mathbf{r},\mathbf{r}')$ can be obtained from the Dyson equation,

$$G_{\sigma_{\mathrm{L}}\sigma_{\mathrm{R}}}(E;\mathbf{r},\mathbf{r}') = G^{(0)}_{\sigma_{\mathrm{L}}\sigma_{\mathrm{R}}}(E;\mathbf{r},\mathbf{r}') + \int d\mathbf{r}_1 G^{(0)}_{\sigma_{\mathrm{L}}\sigma_{\mathrm{R}}}(E;\mathbf{r},\mathbf{r}_1)$$
$$\times H_{\mathrm{imp}}(\mathbf{r}_1)G_{\sigma_{\mathrm{L}}\sigma_{\mathrm{R}}}(E;\mathbf{r}_1,\mathbf{r}'), \tag{2.6}$$

where $G^{(0)}_{\sigma_{\mathrm{L}}\sigma_{\mathrm{R}}}(E;\mathbf{r},\mathbf{r}')$ represents the unperturbed Green's function, it is given by

$$(E - H_0)G^{(0)}_{\sigma_{\mathrm{L}}\sigma_{\mathrm{R}}}(E;\mathbf{r},\mathbf{r}') = \hbar\delta(\mathbf{r}-\mathbf{r}'). \tag{2.7}$$

To solve Eq. (2.7), we can expand the unperturbed GF $G^{(0)}_{\sigma_{\mathrm{L}}\sigma_{\mathrm{R}}}(E;\mathbf{r},\mathbf{r}')$ in the mixed real-space momentum representation,

$$G^{(0)}_{\sigma_{\mathrm{L}}\sigma_{\mathrm{R}}}(E;\mathbf{r},\mathbf{r}') = \frac{1}{A}\sum_{\mathbf{p}}\mathcal{G}_{\sigma_{\mathrm{L}}\sigma_{\mathrm{R}}}(E,\mathbf{p};z,z')e^{-i\mathbf{p}\cdot(\mathbf{y}-\mathbf{y}')}, \tag{2.8}$$

where $\mathbf{y}(\mathbf{y}')$ denotes the coordinate in the xy plane with $\mathbf{p}$ the corresponding lateral momentum, A is the cross-sectional area of the junction, and $\mathcal{G}_{\sigma_{\mathrm{L}}\sigma_{\mathrm{R}}}(E,\mathbf{p};z,z')$ is the z component of $G^{(0)}_{\sigma_{\mathrm{L}}\sigma_{\mathrm{R}}}(E;\mathbf{r},\mathbf{r}')$ at the $\mathbf{p}$ point.

Substituting Eq. (2.8) into Eq. (2.7), one has

$$\left[E+\frac{\hbar^2}{2m}\frac{\partial^2}{\partial z^2}-\frac{\hbar^2\mathbf{p}^2}{2m}-\phi(z)\right]\mathcal{G}_{\sigma_L\sigma_R}(E,\mathbf{p};z,z')=\hbar\,\delta(z-z'). \tag{2.9}$$

The above equation can be solved by connecting $\mathcal{G}_{\sigma_L\sigma_R}(E,\mathbf{p};z,z')$ at the two interfaces, $z=0$ and $z=d$, and also at $z=z'$. It should be noted that the rigorous solution of $\mathcal{G}_{\sigma_L\sigma_R}(E,\mathbf{p};z,z')$ in the barrier will be a linear combination of the Airy functions Ai(z) and Bi(z) since the potential $\phi(z)$ within the barrier is trapezoidal.[8,18] With the help of Airy functions, the $\mathcal{G}_{\sigma_L\sigma_R}(E,\mathbf{p};z,z')$, $G^{(0)}_{\sigma_L\sigma_R}(E;\mathbf{r},\mathbf{r}')$, and $G_{\sigma_L\sigma_R}(E;\mathbf{r},\mathbf{r}')$ obtained above are rigorous and thus is a feasible scheme for investigating the properties of TMR at an arbitrary bias voltage.

After obtaining $G_{\sigma_L\sigma_R}(E;\mathbf{r},\mathbf{r}')$, one will get the transmission wave function $\psi_{R\sigma_R}(\mathbf{r})$ via Eq. (2.5). From $\psi_{R\sigma_R}(\mathbf{r})$, the tunneling current density $J_{\sigma_L\sigma_R}$ can be calculated as follows:[19]

$$J_{\sigma_L\sigma_R}(V)=\frac{e}{2\pi\hbar A}\sum_{\mathbf{p}}\int dE_z T_{\sigma_L\sigma_R}(E,\mathbf{p})[f(E)-f(E+eV)], \tag{2.10}$$

where $E=E_t+E_z$ is the total energy of the tunneling electron, with $E_t=\hbar^2\mathbf{p}^2/(2m)$ and $E_z=\hbar^2k^2_{L\sigma_L}/(2m)$ being the lateral and longitudinal energies; and $T_{\sigma_L\sigma_R}(E,\mathbf{p})$ is the transmission coefficient which is defined as

$$T_{\sigma_L\sigma_R}(E,\mathbf{p})=\frac{1}{A}\int d\mathbf{y}\frac{k_{R\sigma_R}}{k_{L\sigma_L}}|\psi_{R\sigma_R}(\mathbf{r})|^2 \tag{2.11}$$

with

$$k_{L\sigma_L}=\left(\frac{2m}{\hbar^2}\right)^{1/2}\sqrt{E-\frac{\hbar^2\mathbf{p}^2}{2m}+\sigma_L\Delta}, \tag{2.12}$$

$$k_{R\sigma_R}=\left(\frac{2m}{\hbar^2}\right)^{1/2}\sqrt{E-\frac{\hbar^2\mathbf{p}^2}{2m}+eV+\sigma_R\Delta}. \tag{2.13}$$

Here, we note that the lateral effect of the impurity scattering has been included in $T_{\sigma_L\sigma_R}(E,\mathbf{p})$. Finally, the tunneling magnetoresistance can be expressed in terms of $J_{\sigma_L\sigma_R}$,[20]

$$\mathrm{TMR}(V)=\frac{J_{\uparrow\uparrow}(V)+J_{\downarrow\downarrow}(V)-J_{\downarrow\uparrow}(V)-J_{\uparrow\downarrow}(V)}{J_{\uparrow\uparrow}(V)+J_{\downarrow\downarrow}(V)+J_{\downarrow\uparrow}(V)+J_{\uparrow\downarrow}(V)}. \tag{2.14}$$

This formula will be used to study the properties of the TMR at a finite applied voltage.

III. DIRECT TUNNELING AND IMPURITY RESONANCE TUNNELING

In this paper, we shall confine our consideration within the case of dilute doping. For simplicity, the scattering effect in dilute doping will be approximated to the single-impurity problem, that is,

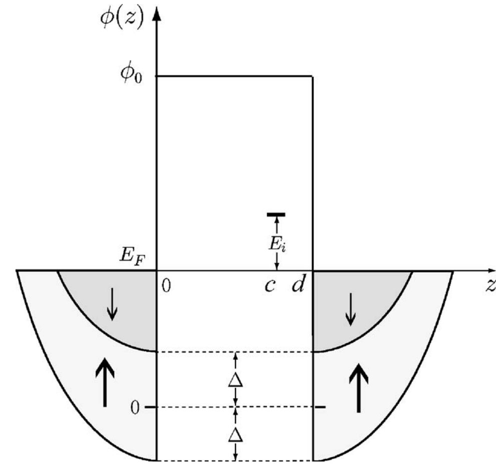

FIG. 1. A schematic potential for the ferromagnetic junction with nonmagnetic impurity locating inside the barrier at zero bias.

$$H_{\mathrm{imp}}(\mathbf{r})=\varepsilon\,\delta(\mathbf{r}-\mathbf{r}_c)=\varepsilon\,\delta(\mathbf{y}-\mathbf{y}_c)\,\delta(z-c), \tag{3.1}$$

where ε is the scattering potential amplitude; $\mathbf{y}_c$ and c are coordinates of impurity in the xy plane and z axis, respectively. Figure 1 shows the spintronic model with a nonmagnetic impurity localized in the barrier at zero bias.

With Eq. (3.1), Eq. (2.6) can be simplified, and thus the transmission wave function of Eq. (2.5) becomes

$$\begin{aligned}\psi_{R\sigma_R}(\mathbf{r})&=i\int d\mathbf{r}'\int\frac{dE}{2\pi}G^{(0)}_{\sigma_L\sigma_R}(E;\mathbf{r},\mathbf{r}')\psi_{L\sigma_L}(\mathbf{r}')\\&\quad+i\int d\mathbf{r}'\int\frac{dE}{2\pi}G^{(0)}_{\sigma_L\sigma_R}(E;\mathbf{r},\mathbf{r}_c)t_{\sigma_L\sigma_R}(E;c)\\&\quad\times G^{(0)}_{\sigma_L\sigma_R}(E;\mathbf{r}_c,\mathbf{r}')k_{L\sigma_L}(\mathbf{r}'),\end{aligned} \tag{3.2}$$

where the t matrix is just the function of c,

$$t_{\sigma_L\sigma_R}(E;c)\equiv t_{\sigma_L\sigma_R}(E;\mathbf{r}_c)=\frac{\varepsilon}{1-\varepsilon G^{(0)}_{\sigma_L\sigma_R}(E;\mathbf{r}_c,\mathbf{r}_c)}. \tag{3.3}$$

On the right-hand side of Eq. (3.2), the first term represents the direct propagation of the electrons from the left electrode to the right electrode, and the second is the indirect propagation via the impurity scattering.

Due to the separation of $\psi_{R\sigma_R}(\mathbf{r})$ into the two parts, the transmission coefficient $T_{\sigma_L\sigma_R}$ defined in Eq. (2.11) will break into three parts: $T_{\sigma_L\sigma_R}=T^{\mathrm{d}}_{\sigma_L\sigma_R}+T^{\mathrm{imp}}_{\sigma_L\sigma_R}+T^{\mathrm{cross}}_{\sigma_L\sigma_R}$. As a result, the tunneling current density $J_{\sigma_L\sigma_R}$ becomes

$$J_{\sigma_L\sigma_R}=J^{\mathrm{d}}_{\sigma_L\sigma_R}+J^{\mathrm{imp}}_{\sigma_L\sigma_R}+J^{\mathrm{cross}}_{\sigma_L\sigma_R}, \tag{3.4}$$

where $J^{\mathrm{d}}_{\sigma_L\sigma_R}$ stands for the direct-tunneling current density, $J^{\mathrm{imp}}_{\sigma_L\sigma_R}$ is the indirect-tunneling current density, and $J^{\mathrm{cross}}_{\sigma_L\sigma_R}$ is the crossing term of direct and indirect tunnelings. As mentioned in the preceding section, for the finite bias case $J^{\mathrm{d}}_{\sigma_L\sigma_R}$, $J^{\mathrm{imp}}_{\sigma_L\sigma_R}$, and $J^{\mathrm{cross}}_{\sigma_L\sigma_R}$ must be expressed in terms of Airy functions Ai(z) and Bi(z). It is thus inconvenient for analytical discussions. On the other hand, the experiments up to

now[9,11,12] are confined only within the low bias region. Therefore we will concentrate ourselves on the low bias case, and employ the Wentzel-Kramers-Brillouin (WKB) approximation to treat the Airy functions.[8,21] We thus find

$$J^{\rm d}_{\sigma_{\rm L}\sigma_{\rm R}} = \frac{e}{2\pi\hbar}\int dE \int \frac{pdp}{2\pi}[f(E)-f(E+eV)] \times \frac{16k_{{\rm L}\sigma_{\rm L}}k_{{\rm R}\sigma_{\rm R}}q_{\rm L}q_{\rm R}e^{-2\int_0^d q(z)dz}}{(k^2_{{\rm L}\sigma_{\rm L}}+q^2_{\rm L})(k^2_{{\rm R}\sigma_{\rm R}}+q^2_{\rm R})}, \quad (3.5)$$

$$J^{\rm imp}_{\sigma_{\rm L}\sigma_{\rm R}} = \frac{1}{A}\frac{2e}{\pi\hbar}\int dE \int [f(E)-f(E+eV)] \times t^{\dagger}_{\sigma_{\rm L}\sigma_{\rm R}}(E;c)t_{\sigma_{\rm L}\sigma_{\rm R}}(E;c)\Phi_{{\rm L}\sigma_{\rm L}}(E;c,V)\Phi_{{\rm R}\sigma_{\rm R}}(E;c,V), \quad (3.6)$$

$$J^{\rm cross}_{\sigma_{\rm L}\sigma_{\rm R}} = -\frac{1}{A}\frac{em}{\pi\hbar^2}\int dE \int \frac{pdp}{2\pi}[f(E)-f(E+eV)] \times {\rm Re}[t_{\sigma_{\rm L}\sigma_{\rm R}}(E;c)]\frac{16k_{{\rm L}\sigma_{\rm L}}k_{{\rm R}\sigma_{\rm R}}q_{\rm L}q_{\rm R}e^{-2\int_0^d q(z)dz}}{q_c(k^2_{{\rm L}\sigma_{\rm L}}+q^2_{\rm L})(k^2_{{\rm R}\sigma_{\rm R}}+q^2_{\rm R})}, \quad (3.7)$$

where $\Phi_{{\rm L}\sigma_{\rm L}}$, $\Phi_{{\rm R}\sigma_{\rm R}}$, and $q(z)$ are defined as follows:

$$\Phi_{{\rm L}\sigma_{\rm L}}(E;c,V) = \frac{1}{\hbar}\int \frac{pdp}{2\pi}\frac{2mk_{{\rm L}\sigma_{\rm L}}q_L}{q_c(k^2_{{\rm L}\sigma_{\rm L}}+q^2_{\rm L})}e^{-2\int_0^c q dz}, \quad (3.8)$$

$$\Phi_{{\rm R}\sigma_{\rm R}}(E;c,V) = \frac{1}{\hbar}\int \frac{pdp}{2\pi}\frac{2mk_{{\rm R}\sigma_{\rm R}}q_R}{q_c(k^2_{{\rm R}\sigma_{\rm R}}+q^2_{\rm R})}e^{-2\int_c^d q dz}, \quad (3.9)$$

$$q(z) = \left(\frac{2m}{\hbar^2}\right)^{1/2}\sqrt{\phi_0 - E + \frac{\hbar^2\mathbf{p}^2}{2m} - \frac{z}{d}eV} \quad (3.10)$$

with $q_{\rm L}=q(0)$, $q_c=q(c)$, and $q_{\rm R}=q(d)$. In arriving at Eqs. (3.5)–(3.9), we have assumed that the summation over $\mathbf{p}$ can be turned into integral, which is proved to be true for a nanojunction with a cross section about 0.01 μm^2.[9]

Equations (3.5)–(3.9) demonstrate that the direct-tunneling current density $J^{\rm d}_{\sigma_{\rm L}\sigma_{\rm R}}$ is irrelevant to the cross section of the junction A, whereas the indirect-tunneling current density $J^{\rm imp}_{\sigma_{\rm L}\sigma_{\rm R}}$ and the cross-tunneling current density $J^{\rm cross}_{\sigma_{\rm L}\sigma_{\rm R}}$ are both inversely proportional to A. The factor $1/A$ appearing in $J^{\rm imp}_{\sigma_{\rm L}\sigma_{\rm R}}$ and $J^{\rm cross}_{\sigma_{\rm L}\sigma_{\rm R}}$ results from the integration over $\mathbf{y}$. Physically, it reflects that the scattering cross section of impurity is directly proportional to the lateral concentration of the impurity. Owing to the inverse proportionality of $J^{\rm imp}_{\sigma_{\rm L}\sigma_{\rm R}}$ and $J^{\rm cross}_{\sigma_{\rm L}\sigma_{\rm R}}$ to A, the larger the junction area is, the weaker the effects of the impurity scattering will be. The effect of the cross section will be discussed in detail in the next section. As will be seen later, by taking into account the effect of the cross section, the experiment results on TMR can be explained in a unified manner.

For the impurity scattering, the most interesting effect is the resonance tunneling. From Eq. (3.3), one can find that the resonance will happen at the condition

$$1 - \varepsilon\,{\rm Re}\left[G^{(0)}_{\sigma_{\rm L}\sigma_{\rm R}}\left(E_i - \frac{c}{d}eV;c,c\right)\right] = 0. \quad (3.11)$$

Following Ref. 13, ${\rm Re}[G^{(0)}_{\sigma_{\rm L}\sigma_{\rm R}}(E;c,c)]$ can be expanded in powers of $[E-E_{\rm i}+(c/d)eV]$. As a result, near the resonance, the indirect-tunneling current density $J^{\rm imp}_{\sigma_{\rm L}\sigma_{\rm R}}$ becomes

$$J^{\rm imp}_{\sigma_{\rm L}\sigma_{\rm R}} = \frac{1}{A}\frac{2e}{\pi\hbar}\int dE[f(E)-f(E+eV)] \times \frac{\Gamma_{{\rm L}\sigma_{\rm L}}(E;c,V)\Gamma_{{\rm R}\sigma_{\rm R}}(E;c,V)}{[E-E_1+eV(c/d)]^2+[\Gamma_{{\rm L}\sigma_{\rm L}}(E;c,V)+\Gamma_{{\rm R}\sigma_{\rm R}}(E;e,V)]^2}, \quad (3.12)$$

where $\Gamma_{{\rm L}\sigma_{\rm L}}(E;c,V) \equiv -\Phi_{{\rm L}\sigma_{\rm L}}(E;c,V)/{\rm Re}G^{(0)\prime}_{\sigma_{\rm L}\sigma_{\rm R}}(E_{\rm i})$, $\Gamma_{{\rm R}\sigma_{\rm R}}(E;c,V) \equiv -\Phi_{{\rm R}\sigma_{\rm R}}(E;c,V)/{\rm Re}G^{(0)\prime}_{\sigma_{\rm L}\sigma_{\rm R}}(E_{\rm i})$, and ${\rm Re}G^{(0)\prime}_{\sigma_{\rm L}\sigma_{\rm R}}(E_{\rm i}) \equiv (\partial/\partial E_{\rm i}){\rm Re}[G^{(0)}_{\sigma_{\rm L}\sigma_{\rm R}}(E_{\rm i}-(c/d)eV;c,c)]$. Note that the second factor within the integrand of Eq. (3.12) represents the well-known Breit-Wigner resonance factor, where the resonance peak locates at the energy $E_{\rm i}-eV(c/d)$ with $\Gamma_{{\rm L}\sigma_{\rm L}}$ and $\Gamma_{{\rm R}\sigma_{\rm R}}$ being its left and the right half widths, respectively.

As for $J^{\rm cross}_{\sigma_{\rm L}\sigma_{\rm R}}$, Eq. (3.7) indicates that $J^{\rm cross}_{\sigma_{\rm L}\sigma_{\rm R}} \propto {\rm Re}[t_{\sigma_{\rm L}\sigma_{\rm R}}(E;c)]$. Because ${\rm Re}[t_{\sigma_{\rm L}\sigma_{\rm R}}(E;c)]$ is a small quantity near the resonance, $J^{\rm cross}_{\sigma_{\rm L}\sigma_{\rm R}}$ is much less than $J^{\rm d}_{\sigma_{\rm L}\sigma_{\rm R}}$ and $J^{\rm imp}_{\sigma_{\rm L}\sigma_{\rm R}}$ in this region. Therefore we can neglect the contribution of $J^{\rm cross}_{\sigma_{\rm L}\sigma_{\rm R}}$ in the neighborhood of resonance,[15] and rewrite Eq. (3.4) as

$$J_{\sigma_{\rm L}\sigma_{\rm R}} = J^{\rm d}_{\sigma_{\rm L}\sigma_{\rm R}} + J^{\rm imp}_{\sigma_{\rm L}\sigma_{\rm R}}. \quad (3.13)$$

At first glance, the resonance factor within Eq. (3.12) is similar to Eq. (1.1). But essentially, Eq. (1.1) is just a simple one-dimensional tunneling theory that does not take into account the lateral effects. When it is applied to simulate experimental data,[9,11,12] $\Gamma_{{\rm L}\sigma_{\rm L}}$ and $\Gamma_{{\rm R}\sigma_{\rm R}}$ are just taken phenomenologically as two different constants, and thus exclude the influences of physical variables, such as the tunneling energy, the impurity position, and the bias voltage. Due to this exclusion and the one-dimensionality of Eq. (1.1), experimental data cannot be well described. In the present theory, we have adopted a three-dimensional picture of tunneling and impurity resonance. The lateral effect of impurity scattering and the influence of relevant physical variables can be easily included in this theory. Therefore it will be more suitable for studying the TMR of nanojunctions.

IV. NUMERICAL RESULTS AND DISCUSSIONS

Because two half linewidths $\Gamma_{{\rm L}\sigma_{\rm L}}$ and $\Gamma_{{\rm R}\sigma_{\rm R}}$ are both the exponential function of c, they are more likely to be of different orders of magnitude. Therefore we will henceforth consider only the asymmetric case, that is, $\Gamma_{{\rm L}\sigma_{\rm L}} \gg \Gamma_{{\rm R}\sigma_{\rm R}}$ if $c < d/2$ or $\Gamma_{{\rm L}\sigma_{\rm L}} \ll \Gamma_{{\rm R}\sigma_{\rm R}}$ if $c > d/2$. The numerical calculations

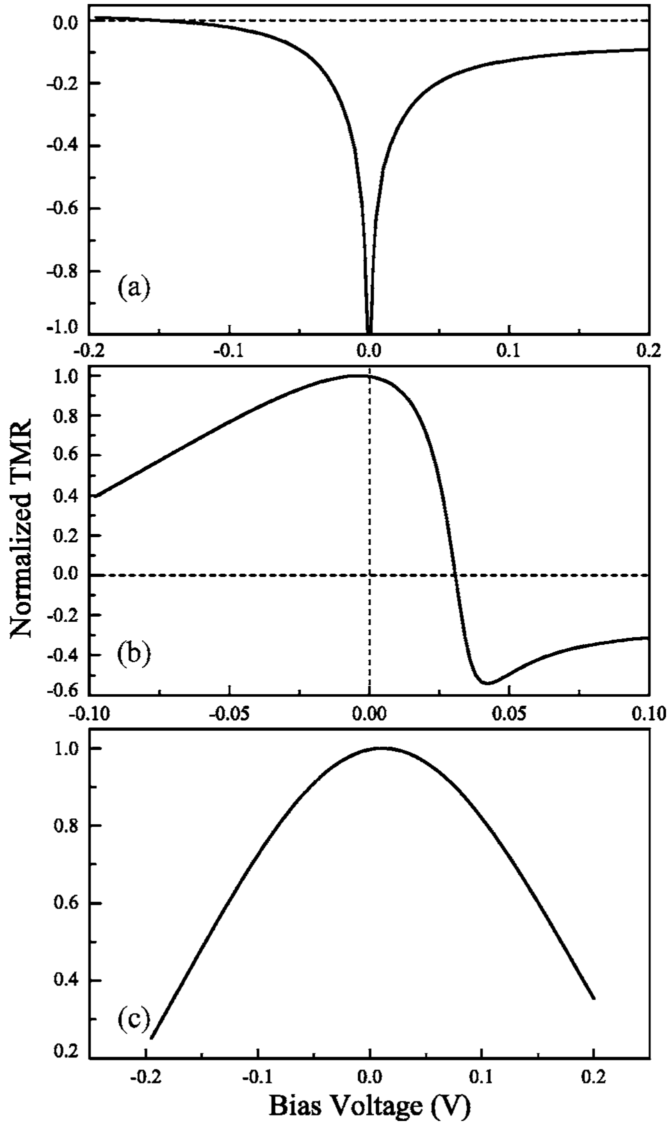

FIG. 2. The curve of normalized TMR vs bias voltage for nanojunctions with (a) $c=21$ Å and $E_i=0$ meV, (b) $c=22$ Å and $E_i=30$ meV, and (c) $c=14$ Å and $E_i=150$ meV.

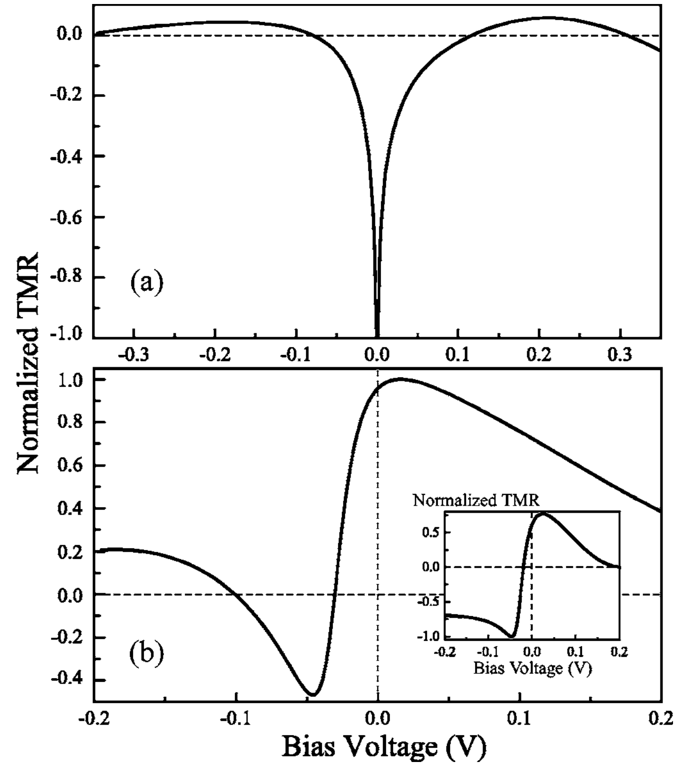

FIG. 3. The curve of normalized TMR vs bias voltage for large-area nanojunctions with (a) $c=21$ Å and $E_i=0$ meV, and (b) $c=2.5$ Å and $E_i=30$ meV. The inset of (b) shows the curve of normalized TMR only considering the indirect tunneling through impurity states. The lateral area density of impurity $x=5\times10^{-4}$ corresponds to 2×10^4 impurities doping in the junction of $A=10$ μm^2.

are performed rigorously according to Eqs. (2.14), (3.5), and (3.6). The numerical results are shown in Figs. 2 and 3. Here, the parameters are chosen as follows: the Fermi level $E_F=2.5$ eV,[22] and the exchange splitting for the FM electrodes $\Delta=2.1$ eV,[22] the barrier width $d=25$ Å, the barrier height $\phi_0-E_F=1.4$ eV, and the energy of impurity state $E_i-E_F=0\sim150$ meV.

A. Indirect tunneling via impurity scattering

In this subsection, we focus on the case where the cross section of junction is so small that the direct tunneling is negligible. The tunneling is now indirect, it comes from the impurity scattering. The numerical results are plotted in Fig. 2 where the impurity level varies relative to the Fermi level of the electrode. In Fig. 2(a), the impurity level lies almost at the Fermi level, the scattering resonance happens near the zero bias, and it results in the inversion of TMR. In Fig. 2(b), the impurity level lies above but not far from the Fermi level, it leads to the resonance and inversion at a finite bias. In contrast to Figs. 2(a) and 2(b), when the impurity level goes far away from the Fermi level, there is no resonance and inversion, TMR decreases with bias but still remains positive, as shown in Fig. 2(c).

Those effects of the impurity level on TMR can be understood qualitatively as follows.

As can be seen from Eqs. (3.8) and (3.9), for the junction with a thick barrier, the main contributions to $\Phi_{L\sigma_L}$ and $\Phi_{R\sigma_R}$ will come from the channel of $\mathbf{p}=0$. We thus approximate $\Gamma_{L\sigma_L}$ and $\Gamma_{R\sigma_R}$ as in Ref. 13,

$$\Gamma_{L\sigma_L}(E;c,V)=\frac{eVk_{L\sigma_L}q_Le^{-2\int_0^c q\mathrm{d}z}}{(k_{L\sigma_L}^2+q_L^2)(q_L-q_c)d}, \tag{4.1}$$

$$\Gamma_{R\sigma_R}(E;c,V)=\frac{eVk_{R\sigma_R}q_Re^{-2\int_c^d q\mathrm{d}z}}{(k_{R\sigma_R}^2+q_R^2)(q_c-q_R)d}. \tag{4.2}$$

Without loss of generality, we assume hereafter $\Gamma_{L\sigma_L}\ll\Gamma_{R\sigma_R}$, i.e., $c\gg d/2$, the impurity lies closer to the right FM electrode. Substituting Eqs. (4.1), (4.2), and (3.12) into Eq. (2.14) and using the Fermi-level approximation,[7] we obtain

$$\mathrm{TMR}(V) = \mathfrak{S}_i(c,V) \times C_L C_R(V) \times P_L P_R(V), \quad (4.3)$$

where

$$\mathfrak{S}_i(c,V) = \frac{[E_i - E_F - eV(c/d)]^2 - \Gamma_{R\uparrow}(E_F;c,V)\Gamma_{R\downarrow}(E_F;c,V)}{[E_i - E_F - eV(c/d)]^2 + \Gamma_{R\uparrow}(E_F;c,V)\Gamma_{R\downarrow}(E_F;c,V)}, \quad (4.4)$$

$$C_L = \frac{q_{FL}^2 - k_{FL\uparrow}k_{FL\downarrow}}{q_{FL}^2 + k_{FL\uparrow}k_{FL\downarrow}} > 0, \quad (4.5)$$

$$C_R(V) = \frac{q_{FR}^2(V) - k_{FR\uparrow}(V)k_{FR\downarrow}(V)}{q_{FR}^2(V) + k_{FR\uparrow}(V)k_{FR\downarrow}(V)} > 0, \quad (4.6)$$

$$P_L = \frac{k_{FL\uparrow} - k_{FL\downarrow}}{k_{FL\uparrow} + k_{FL\downarrow}} > 0, \quad (4.7)$$

$$P_R(V) = \frac{k_{FR\uparrow}(V) - k_{FR\downarrow}(V)}{k_{FR\uparrow}(V) + k_{FR\downarrow}(V)} > 0, \quad (4.8)$$

and the subscript F means that the associated variables take their value at the Fermi level E_F. Here P_L and $P_R(V)$ are the spin polarizations for the left and right electrodes, C_L and $C_R(V)$ are the quantum-coherence factors, and $\mathfrak{S}_i(c,V)$ is the scattering factor representing the effects of impurity resonance. Hereafter, the factors P_L, $P_R(V)$, and C_L are all chosen to be positive, as is the usual case.[6] It should be pointed out that $P_R(V)$ is a slowly varying function of the bias voltage as compared to $C_R(V)$, hence the bias dependence of TMR will be determined mainly by the quantum-coherence factor $C_R(V)$ and the impurity-scattering factor $\mathfrak{S}_i(c,V)$. On the other hand, $C_R(V)$ does not change sign within the measurable range of a few tens of millivolts for impurity-assisted tunneling. Therefore $C_R(V)$ only makes the drop of TMR with increasing bias, whereas $\mathfrak{S}_i(c,V)$ controls the sign change of TMR. It is worth mentioning that besides inverting the sign of the TMR, the localized impurity states in the barrier can also dramatically affect the interlayer exchange coupling, making the coupling much stronger than that in the absence of impurities.[23] However, in this paper we shall concentrate on the sign-change behavior of TMR, and study three tunneling cases according to the impurity energy relative to the Fermi level.[9]

First, when the energy of impurity state matches the Fermi level of the FM electrodes, i.e., $E_i \simeq E_F$, the scattering factor $\mathfrak{S}_i(V=0)=-1$, therefore $\mathrm{TMR}(V=0)=-P_L C_L P_R C_R$, i.e., the TMR becomes negative at zero bias. Near $V=0$, the scattering factor $\mathfrak{S}_i(V)$ will remain negative and increase with V. As a result, the TMR will show a sharp dip within a narrow region near zero bias. This property is clearly shown in Fig. 2(a), it agrees well with the experimental curve shown in Fig. 2(c) of Ref. 9.

Second, when the impurity level E_i lies above the Fermi level E_F but not far away from E_F: $E_i - E_F \gtrsim \sqrt{\Gamma_{R\uparrow}\Gamma_{R\downarrow}}$, TMR displays a sign change at positive bias whereas for the negative bias only the drop of TMR can be observed experimentally.[9] To explain this phenomenon, we should start from the scattering factor of Eq. (4.4), which shows that the inversion of TMR upon positive and negative biases will happen respectively at positive critical voltage V_i and negative critical voltage V_i',

$$\begin{cases} \mathrm{TMR}(V) > 0, & V_i' < V < V_i, \\ \mathrm{TMR}(V) < 0, & V < V_i' \text{ or } V > V_i, \end{cases} \quad (4.9)$$

where

$$V_i = \frac{d}{c}(E_i - E_F - \sqrt{\Gamma_{R\uparrow}\Gamma_{R\downarrow}}) > 0, \quad (4.10)$$

$$V_i' = -\frac{d}{d-c}(E_i - E_F - \sqrt{\Gamma_{R\uparrow}\Gamma_{R\downarrow}}) < 0. \quad (4.11)$$

If the impurity locates more closely to the right electrode, i.e., $c \gg d-c$ ($c \gg d/2$), Eqs. (4.10) and (4.11) show that $|V_i'| \gg V_i$. That is the reason why TMR changes in sign in the positive bias case whereas it does not within the measurable range of bias for the negative case. Furthermore, as was shown in Refs. 6 and 8, the quantum-coherence factor $C_R(V) \propto \phi_0 - (eV + E_z^L) - \sqrt{(E_z^L + eV)^2 - \Delta^2}$, it is a rapid decreasing function of V, and will also cause TMR to decrease with the bias voltage. As a result, both $\mathfrak{S}_i(V)$ and $C_R(V)$ are the originations for the decrease of TMR with the bias voltage. Those analyses are in good agreement with the experimental data of Fig. 2(b) in Ref. 9, within both the positive and negative bias regions. Therefore the present theory overcomes the difficulty of the one-dimensional formula (1.1), which cannot reproduce the drop of TMR occurring at the negative bias voltage.[9]

Third, when the impurity level lies far away from the Fermi level, $E_i - E_F \gg \sqrt{\Gamma_{R\uparrow}\Gamma_{R\downarrow}}$, the impurity resonance cannot take place, the scattering factor $\mathfrak{S}_i(c,V)=1$. As a result,

$$\mathrm{TMR}(V) \simeq C_L C_R(V) \times P_L P_R(V). \quad (4.12)$$

It implies that the TMR will remain positive. Nevertheless, it will decrease significantly as the bias voltage increases, that is because $C_R(V)$ is a rapidly decreasing function of V.[6,8] The above theoretical analyses are in accordance with the numerical results shown in Fig. 2(c), and also agrees quite well with the experimental result of Fig. 2(a) in Ref. 9. Therefore in the case without resonance, the decrease of TMR with bias can be ascribed physically to the quantum-coherence factor of the tunneling electron under the trapezoidal barrier. However, this important factor is absent in Eq. (1.1), that is the reason why it is difficult to reproduce the rapid decrease of TMR with the increasing bias when $E_i - E_F \gg \sqrt{\Gamma_{R\uparrow}\Gamma_{R\downarrow}}$.

To summarize this subsection, TMR is controlled mainly by the impurity-scattering factor if the impurity level matches the Fermi level. It is determined by both the impurity-scattering factor and the quantum-coherence factor if the impurity level lies above but not far away from the Fermi level. It is almost determined by the quantum-coherence factor when the impurity level goes far away from the Fermi level. In short, the present theory can provide a unified explanation to all three different cases of the experiment.[9]

B. Effect of cross section

As stated in Sec. III, the direct-tunneling current density $J^{\mathrm{d}}_{\sigma_{\mathrm{L}}\sigma_{\mathrm{R}}}$ is irrelevant to the cross section of the junction A, whereas the indirect-tunneling current density $J^{\mathrm{imp}}_{\sigma_{\mathrm{L}}\sigma_{\mathrm{R}}}$ is inversely proportional to A. If the junction has a very small cross section, the indirect tunneling will dominate the direct tunneling, and the direct one can be neglected, as has been discussed in the previous subsection. On the contrary, if the junction area A is large enough, the scattering effects of the impurity become negligible, there is only the contribution from the direct tunneling, which corresponds to the common junctions and has been studied in Refs. 6 and 8. When the cross section A of the junction is moderate, the contributions from the direct and indirect tunneling are both nonnegligible, they should be taken into account simultaneously. In this case, the total current density must be written as

$$J_{\sigma_{\mathrm{L}}\sigma_{\mathrm{R}}} = J^{\mathrm{d}}_{\sigma_{\mathrm{L}}\sigma_{\mathrm{R}}} + N_i J^{\mathrm{imp}}_{\sigma_{\mathrm{L}}\sigma_{\mathrm{R}}}, \tag{4.13}$$

where N_i is the number of impurities in the layer $z=c$. Note that we consider only the dilute limit of impurity doping, which corresponds to a very low lateral area concentration of impurities, i.e., $x \ll 1$ ($x \equiv N_i/N$ with N being the number of atoms in the layer $z=c$). As will be seen later, it is sufficient for explaining the experiments of Refs. 11 and 12.

First, let us consider the case of $E_{\mathrm{i}} \simeq E_{\mathrm{F}}$. If the contribution of direct tunneling is omitted, the curve of TMR vs bias voltage has been shown in Fig. 2(a). This curve is different from that in Fig. 4(b) of Ref. 11 when bias voltage increases above 0.2 V. If both the direct and indirect tunneling are taken into account, the numerical results are presented in Fig. 3(a) where the lateral area density of impurity $x=5\times10^{-4}$. It indicates that the TMR is negative near zero bias due to the resonant tunneling through impurity states, and then becomes positive and decreases with the increasing bias because the resonant tunneling vanishes and the direct tunneling dominates the indirect tunneling when the bias voltage is sufficiently high. Obviously, the TMR curve in Fig. 3(a) reproduces the experimental results in Fig. 4(b) of Ref. 11, especially, the two small peaks around $V=\pm0.2$ V. This demonstrates that the indirect and direct tunnelings will compete and cooperate to determine the behavior of TMR if the cross section of the nanojunction gets larger.

Second, in the case of $E_{\mathrm{i}}-E_{\mathrm{F}} \gtrsim \sqrt{\Gamma_{\mathrm{R}\uparrow}\Gamma_{\mathrm{R}\downarrow}}$, if the contribution of direct tunneling is neglected, the TMR will change sign at finite bias voltage, as has already shown in Fig. 2(b). If the impurities are doped near the left electrode, this sign-change behavior would be observed at the negative bias voltage, as shown in the inset of Fig. 3(b). It can be easily found that the inset of Fig. 3(b) and the experimental data in Fig. 3(a) of Ref. 12 are similar but somewhat different. To overcome the difference, we calculate the contributions of both indirect tunneling and direct tunneling, and present the numerical results in Fig. 3(b). Clearly, due to the influence of direct tunneling, the TMR increases rapidly with the increasing negative bias voltage and even changes to a positive value at a large voltage, which agrees with Fig. 3(a) of Ref. 12. Therefore the experimental results on MnAs/GaAs(AlAs)/MnAs large-area nanojunctions[12] can also be naturally explained as the combining effect of direct tunneling and indirect tunneling via impurity states.

To sum up, we have provided a straightforward explanation to the recent experiments on large-area nanojunctions by taking into account the contributions of both the impurity-assisted indirect tunneling and direct tunneling.[11,12]

V. CONCLUSIONS

We have performed a microscopic study of impurity resonance and TMR for magnetic nanojunctions with nonmagnetic impurities in the barrier. The analytical expressions for both the direct and indirect tunnelings are obtained. Within this framework, the lateral effect has been included, and also the TMR can be straightforwardly calculated from the basic physical parameters. It is found that the contributions of direct and indirect tunnelings are controlled by the cross section of the junction. If the cross section is very small, the indirect tunneling will dominate the direct one and the latter is negligible. In this case, the bias dependence of TMR is generally controlled by the impurity-scattering factor $\mathfrak{S}_{\mathrm{i}}$ and quantum-coherence factor C_{R}. If the junction area gets larger, the direct tunneling is nonnegligible and will compete with the indirect tunneling to determine the behavior of TMR. With the above theoretical results, the experiments of nanojunctions are explained in a unified manner.

ACKNOWLEDGMENTS

This project was supported by the State Key Project of Fundamental Research under Grant No. 001CB610602 and the National Science Foundation of China (Grant No. 10474038).

[1] M. Jullière, Phys. Lett. **54A**, 225 (1975).
[2] J. M. de Teresa, A. Barthélémy, A. Fert, J. P. Contour, R. Lyonnet, F. Montaigne, P. Seneor, and A. Vaurès, Phys. Rev. Lett. **82**, 4288 (1999).
[3] E. Y. Tsymbal and D. G. Pettifor, J. Phys.: Condens. Matter **9**, L411 (1997).
[4] E. Y. Tsymbal, O. Mryasov, and P. LeClair, J. Phys.: Condens. Matter **15**, R109 (2003).
[5] M. Sharma, S. X. Wang, and J. H. Nickel, Phys. Rev. Lett. **82**, 616 (1999).
[6] F. F. Li, Z. Z. Li, M. W. Xiao, J. Du, W. Xu, and A. Hu, Phys. Rev. B **69**, 054410 (2004).
[7] J. C. Slonczewski, Phys. Rev. B **39**, 6995 (1989).
[8] Y. Ren, Z. Z. Li, M. W. Xiao, and A. Hu, J. Phys.: Condens. Matter **17**, 4121 (2005).
[9] E. Y. Tsymbal, A. Sokolov, I. F. Sabirianov, and B. Doudin, Phys.

Rev. Lett. **90**, 186602 (2003).
[10] A. I. Larkin and K. A. Matveev, Sov. Phys. JETP **66**, 580 (1987).
[11] J. Varalda, A. J. A. de Oliveira, D. H. Mosca, J.-M. George, M. Eddrief, M. Marangolo, and V. H. Etgens, Phys. Rev. B **72**, 081302(R) (2005).
[12] V. Garcia, H. Jaffrès, M. Eddrief, M. Marangolo, V. H. Etgens, and J.-M. George, Phys. Rev. B **72**, 081303(R) (2005).
[13] A. Vedyayev, D. Bagrets, A. Bagrets, and B. Dieny, Phys. Rev. B **63**, 064429 (2001).
[14] F. Kanjouri, N. Ryzhanova, N. Strelkov, A. Vedyayev, and B. Dieny, J. Appl. Phys. **98**, 083901 (2005).
[15] L. Sheng, D. Y. Xing, and D. N. Sheng, Phys. Rev. B **69**, 132414 (2004).
[16] S. Datta, Superlattices Microstruct. **28**, 253 (2000).
[17] L. I. Schiff, *Quantum Mechanics*, 3rd ed. (McGraw-Hill, New York, 1968).
[18] M. Abramowitz and I. A. Stegun, *Handbook of Mathematical Functions* (Dover, New York, 1965).
[19] E. L. Wolf, *Principles of Electron Tunneling Spectroscopy* (Oxford University Press, New York, 1985).
[20] U. Gafvert and S. Maekawa, IEEE Trans. Magn. **MAG-18**, 707 (1982).
[21] E. Merzbacher, *Quantum Mechanics*, 3rd ed. (John Wiley & Sons, New York, 1998).
[22] M. Stearns, J. Magn. Magn. Mater. **5**, 167 (1977).
[23] M. Y. Zhuravlev, E. Y. Tsymbal, and A. V. Vedyayev, Phys. Rev. Lett. **94**, 026806 (2005).